

Characterizing the groundwater renewability and evolution of the strongly exploited aquifers of the North China Plain by major ions and environmental tracers

Yuanzheng Zhai · Jinsheng Wang · Huan Huan · Jun Zhou · Wang Wei

Received: 3 October 2012 / Published online: 20 January 2013
© Akadémiai Kiadó, Budapest, Hungary 2013

Abstract The Yongding River Alluvial Fan is a north-western part of the North China Plain, at which Beijing is located. Since 1950 and especially 1970, excessive groundwater exploitation has resulted in a significant drop of groundwater table, and it's believed that groundwater will be intensively used continuously in the future. It's essential to reveal the renewability and the evolution of the groundwater for reasonable management, which was achieved based on the analyses of the major ions and environmental tracers in groundwater. According to the dating results of ^3H , CFCs, and ^{14}C , the age of the shallow and deep groundwater was from <5 to 60 a and from <4,000 to >12,000 a, respectively. The recharge rate determined by the groundwater age generally had a decreasing trend from the NW (0.40–1.44 m/a) to the SE (0.07–0.48 m/a). Na and HCO_3^- accumulated from the NW to the SE and the latter was the dominant anion. Chemical modification occurred progressively along the flow paths. The water type of the shallow and deep groundwater changed from Ca–Mg– HCO_3^- to Na– HCO_3^- and from Ca–Mg– HCO_3^- to Ca–Na–Mg– HCO_3^- and Na–Ca–Mg– HCO_3^- from the NW to the SE, respectively. The shallow

groundwater was vulnerable and susceptible to contamination scattered throughout the region, which would probably further extend to the deep groundwater because of the vertical groundwater flow especially through the preferential pathways due to their increasing hydraulic connections.

Keywords Groundwater recharge · Groundwater renewability · Groundwater evolution · Hydrochemistry · Environmental tracer

Introduction

Tracing technique can provide important information on groundwater regime, chemical evolution, and sustainability, and it have made it possible to estimate mean ages of groundwater pumped from wells [1, 2]. In concept, groundwater age dating provides important information on sources and timing recharge and vulnerability of aquifers to contamination [3]. Accordingly, there is growing interest among regulatory agencies in using groundwater age dating to estimate groundwater recharge and map susceptibility of groundwater systems to contamination. Environmental stable and radiogenic isotopes, especially ^2H , ^{18}O , ^3H and ^{14}C activities are invaluable tracers of regional-scale hydrogeological processes [4].

^2H and ^{18}O are the only true tracers of the water molecule and since all processes in the hydrological cycle fractionate $^2\text{H}/^1\text{H}$ and $^{18}\text{O}/^{16}\text{O}$ ratios, $\delta^2\text{H}$ and $\delta^{18}\text{O}$ values may be used to determine the extent of evaporation, recharge conditions (e.g., temperature or altitude), or groundwater mixing [4, 5]. In addition, they are excellent tracers for determining the origin of groundwater [6] and are widely used to study the natural water

Y. Zhai (✉) · J. Wang (✉) · H. Huan · W. Wei
College of Water Sciences, Beijing Normal University,
Beijing 100875, China
e-mail: diszyz@163.com

J. Wang
e-mail: wangjs@bnu.edu.cn

Y. Zhai · J. Wang · H. Huan · W. Wei
Engineering Research Center for Groundwater Pollution Control
and Remediation, Ministry of Education of China,
Beijing 100875, China

J. Zhou
Beijing Institute of Geological Engineering, Beijing 100037,
China

circulation and groundwater movement [7, 8]. Since the early 1960s, isotope techniques have been increasingly applied to hydrological studies, mostly addressed to comprehend the origin of waters [9].

^3H with half-life of 12.32 a, is widely used as a radioisotope tracer to identify the modern groundwater recharge and used for estimation of recent groundwater age [10, 11]. Because the ^3H input function is coupled to the H-bomb peak of 1960s in the world, groundwater with high ^3H concentrations >30 TU (tritium units, 1 TU corresponds to 1 tritium atom per 10^{18} hydrogen atoms of 0.118 Bq/L) indicates a recharge during and after the 1960s [12]. Recent precipitation and recharged groundwater in the northern hemisphere has ^3H values up to 9 TU. The groundwater containing ^3H values <1 TU is often classified as submodern [13]. Very low ^3H values below detection limit mark water samples below baseline of the pre-bomb tests and therefore indicate groundwater residence times of more than 50 a. In contrast, if measurable quantity of ^3H values occurs, modern groundwater age and flow velocity can be determined. Active circulating groundwater and/or dispersion and mixing generally attenuate ^3H values, while less active system may preserve ^3H input of the bomb testing era of nuclear bombs in the atmosphere (1952–1962) [14].

The atmospheric tracer gases CFCs including CCl_3F (CFC-11), CCl_2F_2 (CFC-12) and $\text{C}_2\text{Cl}_3\text{F}_3$ (CFC-113) are increasingly being used as tracers of groundwater age [15] because of their usefulness in dating young groundwater [16]. CFCs are human-made compounds that are stable in the environment. Large-scale production of CFC-12 began in the early 1940s, followed by CFC-11 in the 1950s and by CFC-113 in the 1960s [17]. CFC-11 and CFC-12 were used mainly for refrigeration and air-conditioning, while CFC-113 was used as a solvent. They leaked into the environment with atmospheric concentrations rising from the time of their development in the 1930s until the 1990s, when production was cut back to protect the ozone layer as a result of the Montreal Protocol. CFCs have relatively long residence time in the atmosphere (60, 180 and 85 a, respectively; [18]), and so their atmospheric concentrations are uniform over large years [19] because of their well-mixing in the atmosphere and consequently their input functions are not area-specific as is the case with ^3H [20]. Theoretically the concentrations of these gases in a groundwater can be matched to a particular year of recharge, but in practice there may be complications: some of them have to do with the tracers themselves, while others are related to the fact that groundwater as sampled is probably rarely of a single recharge age, owing to a combination of wellbore and within-aquifer mixing processes [20]. Nevertheless, even where age quantification is not possible the CFCs may be useable as flow tracers [20],

because of their occurrence in groundwater at least indicating a modern groundwater recharge.

In principle, combining groundwater age dates with isotopic characterization and interpretation of chemical composition provides important information on the timing, rate and sources of recharge [21], which in most cases guide assessment of groundwater sustainability [22]. ^{14}C is the most widely used radiometric dating technique for groundwater in regional aquifers [23] and is invaluable in constraining the timescales of groundwater flow and recharge [4], because of its capacity to date groundwater that is up to 10 ka old, and due to the ubiquitous presence of dissolved inorganic carbon (DIC) in groundwater [4, 22]. This technique exploits the decay of ^{14}C from the onset of recharge to estimate groundwater age at locations along the flow path. For ^{14}C dating of groundwater, the initial ^{14}C activity (A_0) at the time of recharge is required as a starting point. Much of the carbon in groundwater is derived from gaseous CO_2 in the vadose zone. However, this carbon, containing high levels of ^{14}C , was diluted by low ^{14}C activity carbon dissolved from minerals during groundwater recharge. For this reason, the estimation of the initial ^{14}C activity (A_0) is difficult [24]. There are several methods of correcting the initial ^{14}C activity for dead-C dilution [25]. These methods considered either only chemical mixing between the carbon compounds, or isotopic fractionation, which was gave a summary overview of the current state-of-art in the radiocarbon dating of groundwater by Geyh [26]. The ^{14}C dating method is not without problems, though many of them have been addressed to minimize uncertainties [22, 27–30].

When coupled with major ion geochemistry and physical hydrogeology, environmental tracers constrain groundwater residence time, distribution and rates of groundwater recharge, water–rock interaction, and groundwater flow paths [5] and are thus fundamental to understanding hydrogeological systems and managing groundwater resources [4]. Environmental tracers have been widely used over the past decades [13, 31–33].

The goal of this work is to study the renewability and the chemical evolution of the groundwater in the Yongding River Alluvial Fan (YRAF) of the North China Plain (NCP) by using the major ions and environmental tracers in the groundwater. The results have important implications for the flow paths, the timing and rate of recharge, the vulnerability, and hence the sustainability of the groundwater.

Study area settings

General setting

As a part of the NCP, the YRAF is located at $39^\circ26'–40^\circ05'\text{N}$ and $116^\circ5'–116^\circ53'\text{E}$ with an area of 2,541 km².

It occupies the middle-southern part of Beijing plain area (Fig. 1). The terrain of the study area gradually becomes lower from northwest to southeast, with average elevation from 60 to 20 m above sea level (masl).

Climatically, the YRAF is affected by the typical continental monsoon climate of northern temperate zone. As a result, there are four distinct seasons. In the winter (December–February), the weather is cold and dry due to northerly winds from high-latitude areas. In the summer (June–August), it is hot and wet because of the east and southeast airflow carrying moisture from the southern Pacific Ocean and the Indian Ocean. The mean annual

precipitation is 585 mm during the past sixty years [34], more than 70 % of which occurs in rainy season during June to August. The long-term average annual potential evaporation is 1,800 mm, which greatly exceeds the annual precipitation. The mean annual temperature is 12 °C.

Hydrogeological setting

The YRAF is bounded by mountainous areas in the northwest, and to the southwest, south, east, and northeast it is open to the NCP. The groundwater is the loose-rock pore water occurring in the Quaternary alluvial aquifer. The

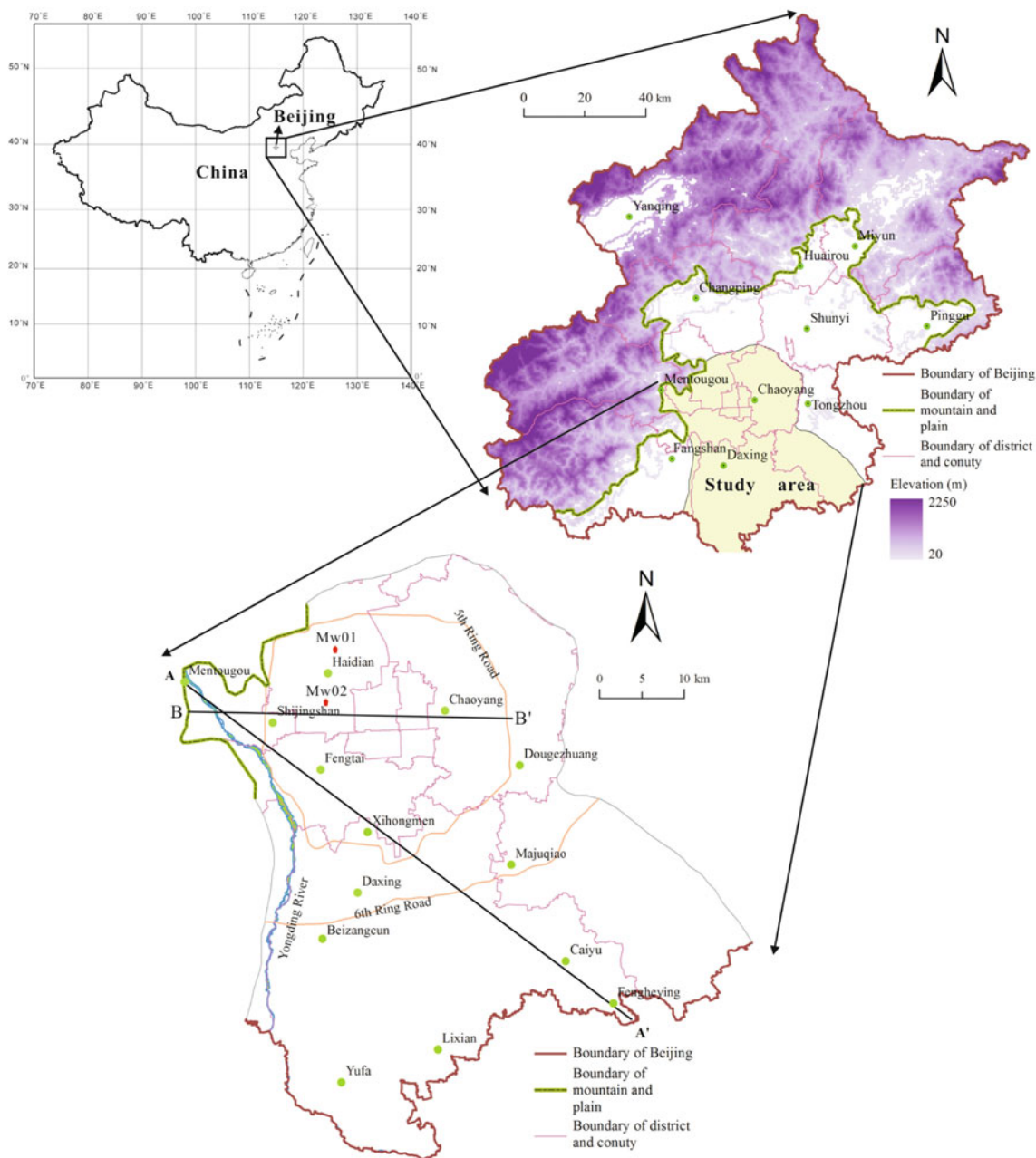


Fig. 1 Location of the study area with the hydrogeological cross sections A–A' and B–B'

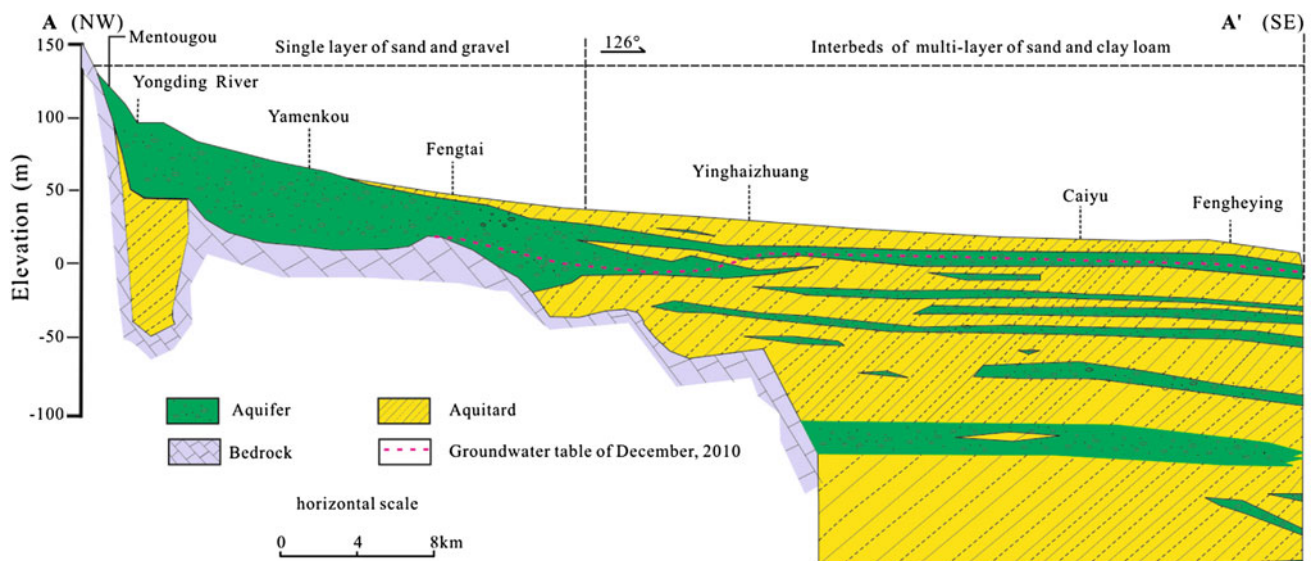


Fig. 2 Hydrogeologic cross section along A–A'

aquifer lithology is primarily gravel and coarse sand in the upstream fan area, and fine and sandy clay in the downstream area (Fig. 2). The present-day aquifer-system occupies the uppermost dozens of meters (northwest) to few hundred meters (southeast) of the sedimentary sequence deposited since Mio-Pliocene time. Hydrostratigraphical analysis indicates thick accumulations of fine to coarse sands with interbedded silt–clay layers of limited lateral extent within the aquifer system. Individual silt–clay layers are variable in thicknesses and depth of occurrence, making lateral correlation inappropriate, but together these silt–clay layers impose a hydraulic anisotropy on the aquifer which plays a vital role in determining patterns of groundwater flow.

The north part of the YRAF is the urban district of Beijing City, where there are a plenty of self-supply pumping wells and several large groundwater sources for urban domestic supply. The south part is mainly dominated by farmland and villages. Winter wheat and summer maize are the major crops, which is largely supported by pumping groundwater resource. Over-pumping of groundwater during the past decades has caused the continuous decline of groundwater table.

Methodology and data

Sampling sites and procedures

Sampling for chemical, ^2H and ^{18}O , ^3H , and CFCs analyses

Sampling for chemical and isotopic analyses was completed in late May–early July 2009. Collected from wells of between 50 m and 200 m depth, 55, 35, 52, and 20

groundwater samples were stored for chemical (K^+ , Na^+ , Ca^{2+} , Mg^{2+} , HCO_3^- , Cl^- , SO_4^{2-} , and NO_3^-), ^2H and ^{18}O , ^3H and CFCs analyses, respectively (Table 1). The distribution of sampling sites is presented in Fig. 3. These wells were screened at the bottoms with screens shorter than 20 m and the rest of them were cemented to ensure groundwater sampling from the specific depth. Wells were pumped at rates less than 2 L per minute to minimize vertical mixing of groundwater during sampling.

A standard, systematically applied sampling procedure was followed for the sampling for chemical, ^2H and ^{18}O , and ^3H analyses. Wells were purged prior to collection of samples. The required purging volume was aimed to be a withdrawal of three borehole volumes of water. In every case a flow-cell for monitoring electrical conductivity (EC), oxidation–reduction potential (ORP) and pH was installed half-way through the well-purging. In all cases stability in the flow-cell readings was achieved, after which water samples were collected. Precautions should be taken to avoid contamination of CFCs of groundwater sample from sampling equipment such as pumps and tubing [35, 36]. This is best tested by using the equipment to sample old waters in which the anthropogenic tracers are known to be below detection. Sample collection by the single bottle method of the USGS [15] is straightforward [20].

Table 1 Numbers and depths of groundwater samples

Parameter	Chemical analysis	^2H and ^{18}O analysis	^3H analysis	CFCs analysis	^{14}C analysis
Sampling number	55	35	52	20	19
Depths (m)	50–200	50–200	50–120	60–120	200–300

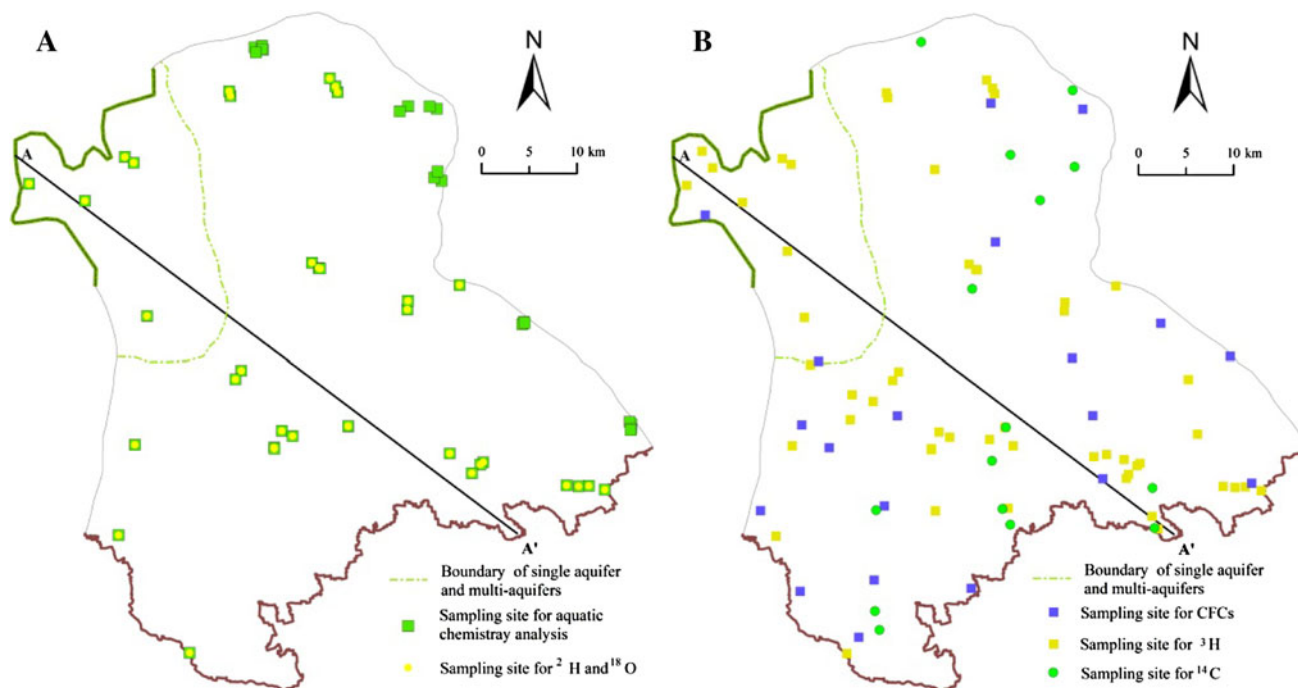


Fig. 3 Sampling sites in the study area

For ^2H and ^{18}O analyses of groundwater, water samples of precipitation in the YRAF in one hydrological cycle (July 2008–July 2009) were also collected, which were analyzed in another paper [37].

Sampling for ^{14}C dating

Sampling for ^{14}C dating was completed in 2005. A total of 19 groundwater samples (Table 1) were collected from wells of between 200 and 300 m depth (Fig. 3b). The sampling procedure was similar to that for other parameter analysis which was just described in the last section. In all cases stability in the flow-cell readings was achieved, after which water samples were collected through 0.25 μm polycarbonate filters along with water samples for stable isotope analysis and ^{14}C activity analysis.

Samples for $^{13}\text{C}/^{12}\text{C}$ and ^{14}C activity determination, the volumes of which were determined according to the HCO_3^- content of groundwater, were collected in thick-walled plastic bottles. To each water sample 0.1–0.2 mL of 1 % Sodium Azide solution was added to prevent biological activities. Groundwater samples remained exposed for 3 min during sampling, before storage in an ice box at the site and subsequently in a freezer.

Measurements

Field measurements

Water temperature (T), dissolved oxygen (DO), EC, ORP, pH, and total dissolved solids (TDS) of groundwater were

measured in the field, all of which were calibrated before use. Other parameters were all measured in labs, and some parameters (such as EC and TDS) were measured again for verification in labs.

Lab measurements

K^+ and Na^+ were determined using a Flame Photometer (GFU-202); Ca^{2+} and Mg^{2+} were determined using EDTA titrimetry. SO_4^{2-} , Cl^- and NO_3^- were determined using Ion Chromatography (HLC-601); HCO_3^- was determined using alkalimetry. The precision and accuracy of analyses of these chemical parameters were tested by running duplicate analyses.

$^2\text{H}/^1\text{H}$ and $^{18}\text{O}/^{16}\text{O}$ were determined using the CO_2 equilibration method and the zinc-reduction method, followed by analysis with a Finnigan MAT 252 mass spectrometer. They were reported in standard δ -notation (‰) representing per mil deviations from the international V-SMOW (Vienna Standard Mean Ocean Water) standard. Precisions for $\delta^2\text{H}$ and $\delta^{18}\text{O}$ were ± 1.0 and ± 0.2 ‰, respectively.

^3H was determined on electrolytically enriched water samples by low-level proportional counting (Quantulus-1220). The results were reported as absolute concentrations in TU with a typical error of ± 1 TU. The detection limit for tritium measurement in the laboratory is about 1 TU.

CFCs were determined by gas chromatography using an electron capture detector (GC-ECD) following cryogenic pre-concentration [15]. The detection limit for CFC

concentrations in water was 0.01 pmol/L with error of less than 5 %. CFC analysis should ideally be calibrated to a bulk air standard collected at an atmospheric monitoring station [20], preferably one of the AGAGE network (<http://www.agage.eas.gatech.edu/>).

^{13}C was determined by mass spectrometry and reported as δ -values related to the V-PDB (Vienna Pee Dee Belemnite) standard. The precision of $\delta^{13}\text{C}$ was ± 0.5 ‰. ^{14}C of dissolved inorganic carbon (DIC) was determined radiometrically by liquid scintillation counter (Quantulus-1220) after conversion to benzene synthesis from carbonates. ^{14}C activity was reported in the unit of percent modern carbon (pMC). The detection limit was 0.7–1.0 pMC.

Results

Groundwater dynamics

Figure 4 illustrate the declining trend of the groundwater table in the typical hydrogeologic profile during the past decades in the YRAF. Because the area is lack of local surface water bodies, the only available water resource for domestic supply and irrigation is groundwater. In the recent decades the natural groundwater dynamics has been greatly affected by the intensive abstraction related to irrigation, industrial, urban and drinking purposes. Since 1950 and especially 1970, groundwater has been extensively

exploited, resulting in a significant drop of the groundwater table. In present, the depth to the water table is more than 30 m in the northwest (NW) and 20 m in the southeast (SE) (Fig. 4). The mean depth to water table in 2008 has declined by 5.62 and 15.42 m from 1.88 and 7.50 to 22.92 m since 1962 and 1981, respectively. According to the function between the groundwater reservoir and table in the Beijing Plain, the equivalent specific yield in the YRAF is 0.077 [38]. Based on the information, the loss of the groundwater reservoir has reached about 30×10^8 and $41 \times 10^8 \text{ m}^3$ in 2008 since 1981 and 1962, respectively. That is to say, the mean groundwater table declines with a speed of 0.30 and 0.57 m/a during period 1962–1981 and 1981–2008, respectively, and the groundwater reservoir decreases by 0.58×10^8 and $1.11 \times 10^8 \text{ m}^3/\text{a}$ during period 1962–1981 and 1981–2008, respectively.

Aquatic chemistry

The pH of the groundwater ranges from 5.0 to 7.4 with the mean of 6.1, which indicates a slightly acid environment. The TDS of the groundwater ranges from 203.0 to 1,608.0 mg/L with the mean of 462.6 mg/L, and the EC increases correspondingly from 420.0 to 3,140.0 $\mu\text{s}/\text{cm}$ with the mean of 954 $\mu\text{s}/\text{cm}$, having a well positive correlation with the TDS ($R^2 = 0.9997$). The groundwater chemistry with depth and along paths of the groundwater flow is studied. The variations of pH and TDS with the

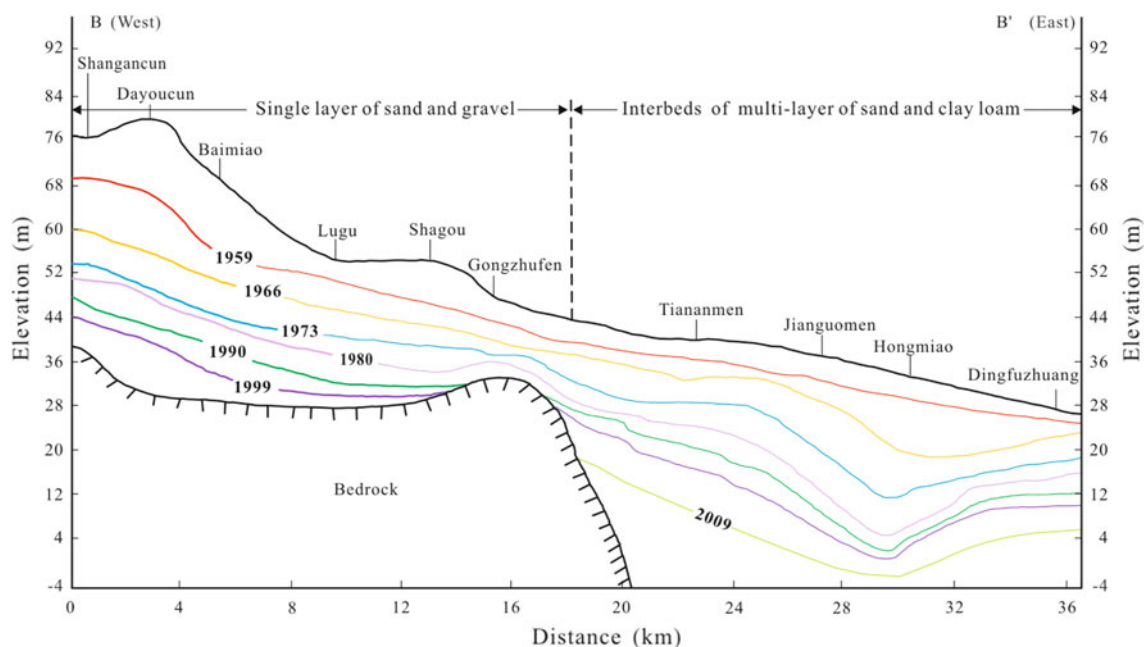


Fig. 4 Groundwater table regime during the past decades observed along cross section B–B'

distance from the piedmont are presented in Fig. 5a, b, both of which indicate that they generally increase from the NW to the SE. The chemical types of the samples are presented in the Piper plot (Fig. 6). Trends of the groundwater chemistry from the NW to the SE may give clues to the evolution prevailing in the YRAF, which will be discussed later in the “Groundwater chemical evolution” section.

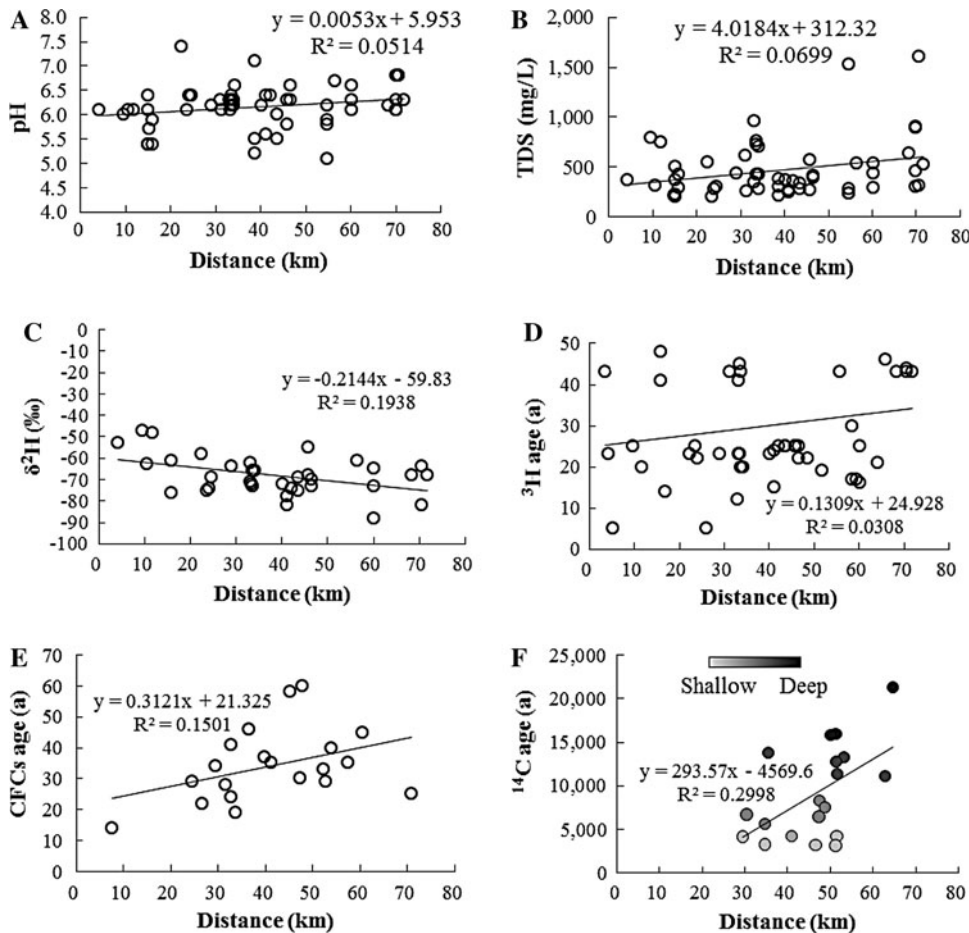
$\delta^2\text{H}$ and $\delta^{18}\text{O}$

The shallow groundwater has $\delta^2\text{H}$ and $\delta^{18}\text{O}$ values in the range of -75.0 to -47.0 ‰ and -10.1 to -5.0 ‰, respectively. The deep groundwater has $\delta^2\text{H}$ and $\delta^{18}\text{O}$ values in the range of -88.0 to -66.0 ‰ and -11.7 to -8.8 ‰, respectively. The average values of $\delta^2\text{H}$ and $\delta^{18}\text{O}$ of the shallow and deep groundwater are -63.9 and -8.5 ‰, and -75.2 and -9.9 ‰, respectively. $\delta^2\text{H}$ and $\delta^{18}\text{O}$ values of shallow and deep groundwater with the world meteoric water line (WMWL; [39]) and the local meteoric water line (LMWL; [37]) are plotted in Fig. 7. The variation of $\delta^2\text{H}$ with the distance from the piedmont and the variation of $\delta^{18}\text{O}$ with depth are presented in Figs. 5c and 8, respectively.

^3H

All groundwater samples for ^3H analysis were collected with depths ranging from 50 to 120 m, which were considered to represent the shallow groundwater in the YRAF. ^3H values measured are in the range of 2.12–47.00 TU, which generally exhibit a decreasing trend from the NW to the SE and decrease with increasing depth. The ^3H values with depths of more than 100 m from ground are <5.00 TU, which indicates that the groundwater at these depths is with the background level of stratum. In contrast, the ^3H values with depths of less than 100 m from ground are generally in the range of 5.00–47.00 TU. ^3H ages of the shallow groundwater were calculated by using the dating model used by Sarra et al. [40]. The age represents the time it has taken groundwater to flow from the water table (recharge location) to the sampling point. The variation of the groundwater age determined by ^3H with the distance from the piedmont is presented in Fig. 5d, which shows that the shallow groundwater generally becomes older from the NW to the SE and is from 5 to 60 a with the average age of 30 a. Further analysis of the shallow groundwater based on ^3H age will be made combined with CFCs age in the last paragraph of the following section.

Fig. 5 Variations of **a** pH, **b** TDS, **c** $\delta^2\text{H}$, **d** ^3H age, **e** CFCs age, and **f** ^{14}C age with distance from the NW piedmont



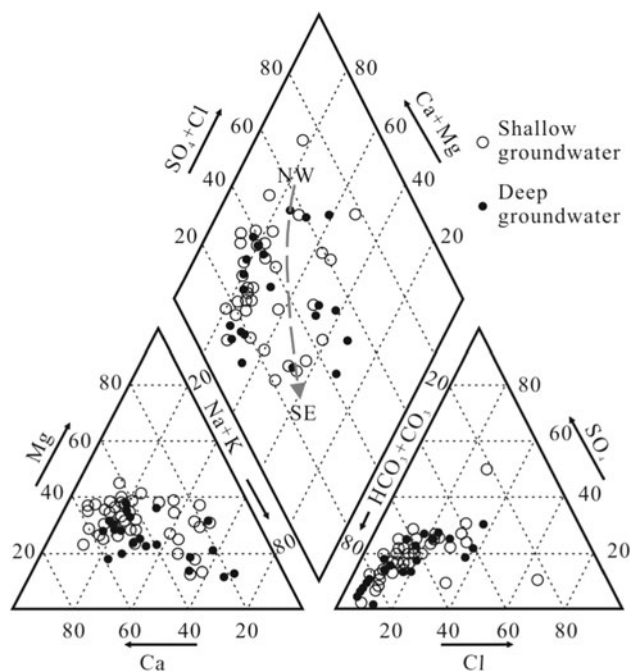


Fig. 6 Piper diagram for the major ions in groundwater

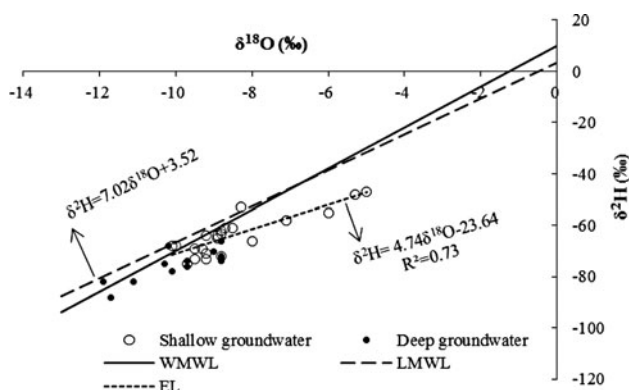
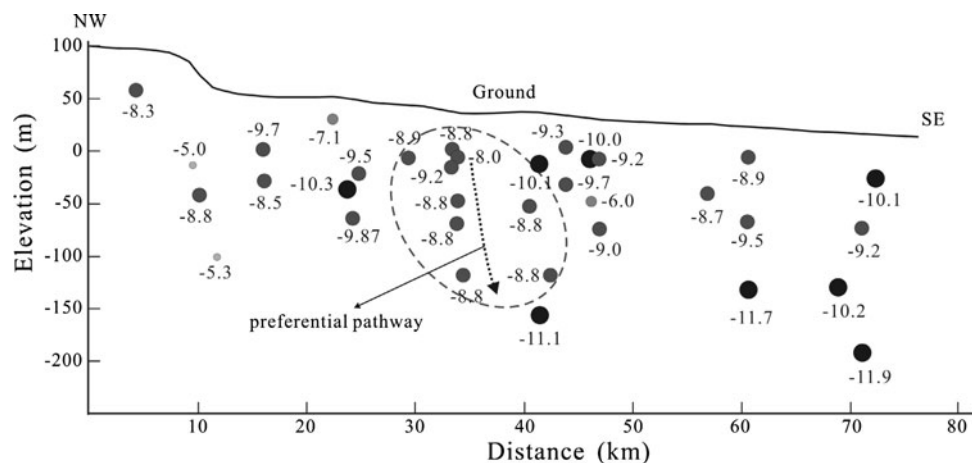


Fig. 7 Plot of $\delta^2\text{H}$ and $\delta^{18}\text{O}$ for shallow and deep groundwater

Fig. 8 Variation of $\delta^{18}\text{O}$ (‰) with depth and distance



CFCs

The use of CFCs in groundwater as indicators of residence time is based on the known rise of their concentrations in the atmosphere over the past 60 a, the observation that they are well-mixing in the atmosphere, and the assumption that they dissolve in water according to their Henry's Law solubilities at the temperature of recharge [3, 41]. The curves of CFCs in northern hemisphere established by Darling et al. [20] are adopted in this work, which can be considered feasible based on the phenomenon discovered in Beijing by Barletta et al. [42]. The assumptions of CFC dating model include that the travel time of CFCs in the unsaturated zone can be neglected, the movement of CFCs is consistent with groundwater, and CFCs don't degrade over time. Dating processes are not introduced here, and CFC apparent ages are determined using the method developed by Plummer et al. [43]. CFCs concentration generally decreases from the NW to the SE and decreases with increasing depth, especially CFC-12 and CFC-13. The variation of CFCs age with the distance from the piedmont is presented in Fig. 5e, which shows that the groundwater age determined by CFCs is in the range of 10 to 60 a with the mean of 34 a, which is similar to that determined by ^3H (from 5 to 60 a). It can be inferred that the groundwater in these depths were recharged by the modern precipitation infiltration during the past decades, and modern water is more likely to participate in the groundwater circulation from the SE and to NW because of more local recharge by stream and rain water through more permeable unconsolidated sediments.

The short residence time of groundwater combinedly determined by ^3H and CFCs indicates a rapid circulation of the shallow groundwater, the horizontal distribution of age isoline of which is shown in Fig. 9a. It can be seen from Fig. 9a that, the spatial distribution of the isoline density (more intensive from the NW to the SE) can roughly reflect

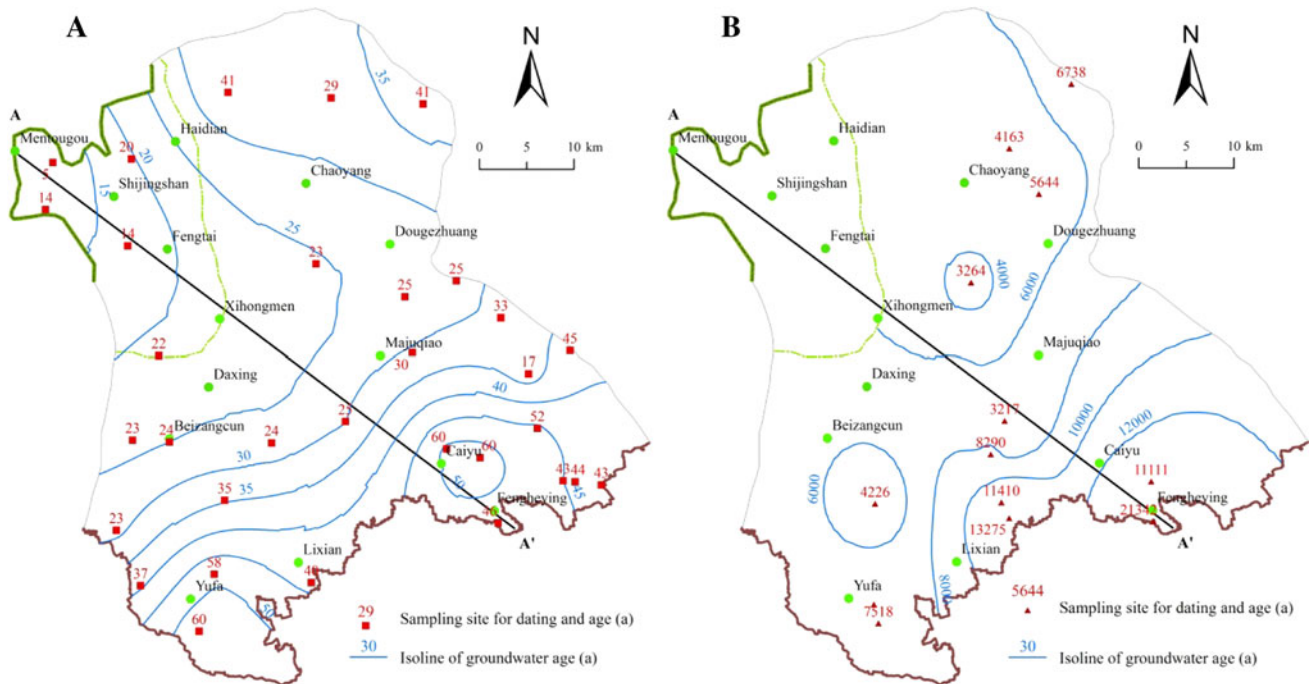


Fig. 9 Horizontal distribution of isoline of **a** Shallow groundwater age and **b** Deep groundwater age

the distribution of the flow velocity: the more sharply age increases, the more slowly water migrates.

¹⁴C

Fontes–Garnier ¹⁴C-DIC Model [27] is adopted in this work, the ages determined by which were considered to be the most representative in the NCP [44]. The use of ¹⁴C as a sole age determinant in the deep groundwater system is complex and probably debatable. However, ¹⁴C data can be used as a powerful tool for better understanding the processes involving the carbonate system and for yielding a rough timescale [23]. The variation of the deep groundwater age determined by ¹⁴C with the distance from the NW to the SE is presented in Fig. 5f, which shows that the deep groundwater generally becomes older and are from 3,150 to 21,342 a with the average age of 9,072 a.

The horizontal distribution of isoline of the deep groundwater age determined by ¹⁴C is shown in Fig. 9b. Figure 9 indicates that, the circulation of the shallow groundwater probably takes place within one hundred years, while that of the deep groundwater is probably over thousands of years and even much longer, both of which present a general trend of increasing age with distance from the NW.

Discussion

Environmental tracers have allowed an understanding of hydrogeochemical processes and regional groundwater flow

in the YRAF that was difficult if not possible from a consideration of physical parameters and major ion chemistry alone.

Groundwater origin

The groundwater in the deep aquifers is characterized by relatively depleted δ²H and δ¹⁸O (−9.9 and −75.2 ‰, respectively) with respect to modern recharge in the shallow aquifers (−8.5 and −63.9 ‰, respectively), and the intersection point of the evaporation line (EL) and the WMWL falls at the bottom left of the WMWL (Fig. 7), which indicates that it was probably recharged during a colder climate in the Pleistocene [45], which is also proved due to non-detection of ³H and a low content of ¹⁴C (<10 pMC). Nevertheless, δ²H and δ¹⁸O values of deep groundwater are generally smaller than modern surface water (−6.3 and −49.5 ‰, respectively; [46]) and precipitation (−5.1 and −38.4 ‰, respectively; [46]), which suggest that it was recharged from surface water and precipitation radically during the long historical period with evaporation processes, which can be further quantified by using groundwater age data.

The abnormal distribution of δ¹⁸O with the depth suggest that the groundwater dynamics in the strongly exploited aquifers (enclosed by the dashed line in Fig. 8) may be affected by transient leakage from the overlying aquifers through the aquitards, the mechanism of which may need to be further revealed by using other means, such as environmental tracing techniques.

Groundwater recharge rate

Recharge in all catchments occurs across broad areas is unconfined [4] and complex [1], which is also proved in the YRAF in this work. It can be seen from Fig. 5b, d, e, f that, groundwater contain higher salinity (TDS) with older ages while lower salinity with younger ages. The gravel and coarse sand sediments in the NW result in relatively lower degrees of evapotranspiration and salinity, and higher recharge rates, and as a first approximation groundwater salinity can be considered as an indication of relative recharge rates.

Recharge rates may be calculated using the ages determined by ^3H , CFCs and ^{14}C , because a groundwater's age is closely related to the rate it migrates [1]. Considering simple migration in one dimension, flow velocity is the reciprocal of the age gradient, which is the rate that age changes with distance along the direction of flow [1]. Although the trends of increasing age with depth and horizontal distance are irregular in practice, probably because the groundwater flow is influenced strongly by hydraulic anisotropy imposed by discontinuous low permeability layers interbedded within the aquifer [47], groundwater with different ages commonly occurs at different depths and distances. The general trends of age with depth and horizontal distance imply flow velocities of approximately 2.5–6.0 m/a in the NW (specific yield of 0.16–0.24) and 1.3–3.0 m/a in the SE (specific yield of 0.05–0.16) of the shallow aquifers, and approximately 0.38 m/a of the deep aquifers (specific yield of 0.01–0.05). These flow velocities equate to recharge rates of 0.40–1.44, 0.07–0.48, and 0.004–0.019 m/a, respectively. The recharge rates (Darcian velocity) of the shallow aquifers are similar to those during the period 1981–2008 estimated by dynamic equilibrium method (DEM; [38]), the comparison of which are given in Table 2.

A similar work [48] was done in another region of the NCP, Shijiazhuang City, the capital of the Hebei Province, 200 km south away from the YRAF, which is under a very similar natural and social condition to the YRAF. An effective recharge rate of around 0.30 m/a was obtained by

Table 2 Comparison of recharge rates calculated by different methods

Parameter	NW	SE	DA
Flow velocity determined by age (m/a)	2.5–6.0	1.3–3.0	0.38
Specific yield	0.16–0.24	0.05–0.16	0.01–0.05
Recharge rate determined by age (m/a)	0.40–1.44	0.07–0.48	0.004–0.019
Recharge rate determined by DEM (m/a)	0.49–0.84	0.15–0.46	–

using ^3H and ^3He as environmental tracers for this region, which is similar to the recharge rates of the YRAF.

Groundwater chemical evolution

Both of the quality and the spatial–temporal chemical evolution of groundwater are determined by major ions sodium, calcium, magnesium, and chloride. The Piper plot (Fig. 6) shows the relationship among the major ions and reiterates that the majority of the groundwater chemistry consists of Ca, Na, Mg, HCO_3 , and SO_4 , from which it also can be inferred that Na and HCO_3 accumulate from the NW to the SE. It's also worth noting that HCO_3 is the dominant anion in most of the groundwater samples. In general, chemical modification of groundwater occurs progressively along flow paths following recharge; the longer the flow path and the travel time, the greater the hydrochemical maturation [49]. The water type of the shallow groundwater in the YRAF changes from Ca–Mg– HCO_3 type to Na– HCO_3 type from the NW to the SE, while that of the deep groundwater changes from Ca–Mg– HCO_3 type to Ca–Na–Mg– HCO_3 and Na–Ca–Mg– HCO_3 type, both of which conform to such a systematically linear pattern. The phenomenon indicates that, ion dissolution and exchange between the groundwater and the media profoundly modify the chemical composition of the groundwater along the flow paths, which are the major processes controlling the chemical composition and evolution of the groundwater.

The slope of the EL (4.74, Fig. 7) indicates that the groundwater is enriched in ^{18}O and less in ^2H in comparison with the WMWL. This phenomenon may also indicates that, complex water–rock exchange processes are influencing the groundwater signature as that known for sedimentary rocks such as brines and solutions in contact with clay layers.

Sustainability implications

The groundwater in the YRAF is locally used for agricultural irrigation, industrial supply, and especially for increasing domestic supply. Population and economic activity in this region are increasing quickly, and the population of Beijing has exceeded 20 million by the end of 2011, which is located at the region. As the capital of China, Beijing is the nation's political, economic and cultural center as well as Chinese most important center for international contacts. This increased activity and the realization that the local surface water has been fully allocated mean that groundwater will be used increasingly for water supply. However, the results of this work indicate that, the exploitation intensity is overwhelming the recharge rate of groundwater, and the aquifers are with a continuously decreasing reservoir during the past decades,

which can be seen obviously in Fig. 4. Additionally, given the broad recharge areas and short residence time, the shallow groundwater in the YRAF is susceptible to contamination from agricultural activities, urban discharge, and the numerous industries scattered throughout the region, which will probably further extend to the deep groundwater because of the vertical groundwater flow. Predicting exactly where these impacts are most likely, however, is difficult because the heterogeneous nature of the YRAF results in localized pathways of preferential flow. Lateral hydraulic gradients and vertical hydraulic connections among different aquifers in the YRAF are increasing quickly due to the increasing extension of the cone of depression of the groundwater table, which can be probably proved by the abnormal vertical distribution of $\delta^{18}\text{O}$ values at the location enclosed by the dashed line in Fig. 8. Excessive groundwater extraction may also cause contaminated water through the preferential pathways in the YRAF, like that drawn in Fig. 8.

Conclusions

According to the dating results of ^3H , CFCs, and ^{14}C , the age of the shallow and deep groundwater was from <5 to 60 a and from <4,000 to >12,000 a, respectively. Despite uncertainties in the interpretation of the age results, it probably could be concluded that the shallow groundwater in the YRAF was mainly recharged by modern precipitation within the past 100 years. In contrast, the deep groundwater was recharged from precipitation radically during the long historical period with evaporation processes during a colder climate in the Pleistocene. The recharge rate determined by groundwater age generally had a decreasing trend from the NW (0.40–1.44 m/a) to the SE (0.07–0.48 m/a), which was similar to that determined by DEM and to that of another region of the NCP, Shijiazhuang City, 200 km south away from the YRAF. Ion dissolution and exchange between the groundwater and the media profoundly modified the chemical composition of the groundwater along the flow paths, which were the major processes controlling the chemical composition and evolution of the groundwater. Na and HCO_3 accumulated from the NW to the SE and the latter was the dominant anion in most of the groundwater samples. Chemical modification occurred progressively along the flow paths. The water type of the shallow and deep groundwater changed from Ca–Mg– HCO_3 to Na– HCO_3 and from Ca–Mg– HCO_3 to Ca–Na–Mg– HCO_3 and Na–Ca–Mg– HCO_3 from the NW to the SE, respectively. The shallow groundwater was vulnerable and susceptible to contamination scattered throughout the region, which would probably further extend to the deep groundwater because of

the vertical groundwater flow especially through the preferential pathways due to their increasing hydraulic connections. Nevertheless, it needed further investigation to quantify the preferential and exchange processes.

Acknowledgments This project was funded by Beijing Municipal Science & Technology Commission (NO. D07050601510000), China. Thanks are due to Beijing Water Authority. We also thank all of the technical reviewers and editors of this manuscript.

References

- Bethke CM, Johnson TM (2008) Groundwater age and groundwater age dating. *Annu Rev Earth Planet Sci* 36:121–152
- Pavel PP (2012) Recent developments in radioanalytical technologies for environmental investigations. *J Radioanal Nucl Chem*. doi:10.1007/s10967-012-1805-z
- Gary SW, Zhang Y, Eric ML, Graham EF (2002) Dispersion of groundwater age in an alluvial aquifer system. *Water Resour Res* 38(10):1198–1211
- Ian C, Tamie RW, Dioni IC, Fifield LK, Sarah OT, Ben P, Ian S (2012) Constraining groundwater flow, residence times, inter-aquifer mixing, and aquifer properties using environmental isotopes in the southeast Murray Basin. *Aust Appl Geochem* 27(9): 1698–1709
- Edmunds W (2009) Geochemistry's vital contribution to solving water resource problems. *Appl Geochem* 24(6):1058–1073
- Zhao LJ, Xiao HL, Dong ZB, Xiao SC, Zhou MX, Cheng GD, Yin L, Yin ZL (2012) Origins of groundwater inferred from isotopic patterns of the Badain Jaran desert Northwestern China. *Ground Water* 50(5):715–725
- Chen ZY, Wei W, Liu J, Wang Y, Chen J (2011) Identifying the recharge sources and age of groundwater in the Songnen Plain (Northeast China) using environmental isotopes. *Hydrogeol J* 19(1):163–176
- Wang JS, Zuo R, Teng YG, Hu QH, Sun ZJ (2010) Sorption of strontium and fractal scaling of the heterogeneous media in a candidate VLLW disposal site. *J Radioanal Nucl Chem* 283:319–328
- Minissale A, Vaselli O (2011) Karst springs as “natural” pluviometers: constraints on the isotopic composition of rainfall in the Apennines of central Italy. *Appl Geochem* 26(5):838–852
- Yoon YY, Seung GL, Tong KK, Tae JL, Kil YL (2012) Radio-nuclides analysis in hot spring waters in Korea by liquid scintillation counting. *J Radioanal Nucl Chem* 294(2):209–213
- Uwe M, Christopher JD (2012) Groundwater age for identification of baseline groundwater quality and impacts of land-use intensification-The National Groundwater Monitoring Programme of New Zealand. *J Hydrol* 456–457:79–93
- Mashaikhi K, Oswald S, Attinger S, Buchel G, Knoller K, Strauch G (2012) Evaluation of groundwater dynamics and quality in the Najd aquifers located in the Sultanate of Oman. *Environ Earth Sci* 66(4):1195–1211
- Clark DI, Fritz P (1997) Environmental isotopes in hydrogeology. Lewis, New York, p 328
- Moctar D, Serigne F, Willibald S, Piotr M (2012) Isotopic and geochemical characteristics of groundwater in the Senegal River delta aquifer: implication of recharge and flow regime. *Environ Earth Sci* 66(4):1011–1020
- IAEA (2006) Use of chlorofluorocarbons in hydrology: a guidebook, STI/PUB/1238. http://www-pub.iaea.org/MTCD/publications/PDF/Pub1238_web.pdf

16. Oster H, Sonntag C, Munnich KO (1996) Groundwater age dating with chlorofluorocarbons. *Water Resour Res* 32(10):2989–3001
17. Gholam A, Jay H, Pierre P (2006) Groundwater age. Wiley, New Jersey, p 325
18. Cunnold DM, Fraser PJ, Weiss RF, Prinn RG, Simmonds PG, Miller BR, Alyea FN (1991) Crawford AJ (1994) Global trends and annual releases of CCl₃F and CCl₂F₂ estimated from ALE/GAGE and other measurements from July 1978 to. *J Geophys Res* 99(D1):1107–1126
19. Cook PG, Solomon DK (1997) Recent advances in dating young groundwater: chlorofluorocarbons, ³H/³He and ⁸⁵Kr. *J Hydrol* 191(1–4):245–265
20. Darling WG, Goody DC, MacDonald AM, Morris BL (2012) The practicalities of using CFCs and SF₆ for groundwater dating and tracing. *Appl Geochem* 27(9):1688–1697
21. Madaubuchi C, Faye S, Maloszewski P (2006) Isotope evidence of palaeorecharge and palaeoclimate in the deep confined aquifers of the Chad Basin, NE Nigeria. *Sci Total Environ* 370(2–3):467–479
22. Mohammad AH, William GB (2012) ¹⁴C dating of deep groundwater in the Bengal Aquifer System, Bangladesh: implications for aquifer anisotropy, recharge sources and sustainability. *J Hydrol* 444–445:209–220
23. Avrahamov N, Yechieli Y, Lazar B, Lewenberg O, Boaretto E, Sivan O (2010) Characterization and dating of saline groundwater in the Dead Sea area. *Radiocarbon* 52(3):1123–1140
24. Chen ZY, Nie ZL, Zhang GH, Wan L, Shen JM (2006) Environmental isotopic study on the recharge and residence time of groundwater in the Heihe River Basin, northwestern China. *Hydrogeol J* 14(8):1635–1651
25. Vogel JC (1970) Carbon-14 dating of groundwater. In: isotope hydrology. IAEA, Vienna, pp 225–239
26. Geyh MA (2000) An overview of ¹⁴C analysis in the study of groundwater. *Radiocarbon* 42(1):99–114
27. Fontes JC, Garnier JM (1979) Determination of the initial ¹⁴C activity of the total dissolved carbon: a review of the existing models and a new approach. *Water Resour Res* 15(2):399–413
28. Aravena R, Wassenaar LI, Plummer LN (1995) Estimating ¹⁴C groundwater ages in a methanogenic aquifer. *Water Resour Res* 31(9):2307–2317
29. Coetsiers M, Walraevens K (2009) A new correction model for ¹⁴C ages in aquifers with complex geochemistry-application to the Neogene Aquifer, Belgium. *Appl Geochem* 24(5):768–776
30. Cartwright I (2010) Using groundwater geochemistry and environmental isotopes to assess the correction of ¹⁴C ages in a silicate-dominated aquifer system. *J Hydrol* 382(1–4):174–187
31. Weaver T, Bahr J (1991) Geochemical evolution in the Cambrian-Ordovician Sandstone Aquifer, eastern Wisconsin. 2. Correlation between flow paths and groundwater chemistry. *Ground Water* 29(4):510–515
32. Boronina A, Balderera W, Renard B, Stichler W (2005) Study of stable isotopes in the Kouris Catchment (Cyprus) for the description of regional groundwater flow. *J Hydrol* 308(1–4):214–226
33. Zhai YZ, Wang JS, Teng YG, Zuo R (2012) Hydrogeochemical and isotopic evidence of groundwater evolution and recharge in aquifers in Beijing Plain, China. *Environ Earth Sci.* doi:10.1007/s12665-012-2045-9
34. Zhai YZ, Wang JS, Teng YG, Zuo R (2012) Water demand forecasting of Beijing using the Time Series Forecasting Method. *J Geogr Sci* 22(5):919–932
35. Dunkle SA, Plummer LN, Busenberg E, Phillips PJ, Denver JM, Hamilton PA, Michel RL, Coplen TB (1993) Chlorofluorocarbons (CCl₃F and CCl₂F₂) as dating tools and hydrologic tracers in shallow groundwater of the Delmarva Peninsula, Atlantic Coastal Plain, United States. *Water Resour Res* 29:3837–3860
36. Cook PG, Solomon DK (1995) Transport of trace gases to the water table: implications for groundwater dating with chlorofluorocarbons and krypton-85. *Water Resour Res* 31:263–270
37. Zhai YZ, Wang JS, Teng YG, Zuo R (2011) Chemical and isotopic characteristics of groundwater in the Yongding river groundwater system of Beijing plain. *Acta Geoscientica Sinica* 32(1):101–106
38. Zhai YZ, Wang JS (2012) Temporal variations of elements of groundwater regime in Beijing Plain and its implications. *J Hydraul Eng* 43(9):1034–1041
39. Craig H (1961) Isotopic variations in meteoric waters. *Science* 133:1702–1703
40. Sarra BHS, Najiba C, Kamel Z, Anne LCP, Vincent V, Vincent M (2012) Natural and artificial recharge investigation in the Zeroud Basin, Central Tunisia: impact of Sidi Saad Dam storage. *Environ Earth Sci* 66(4):1099–1110
41. Plummer LN, Busenberg E (1999) Chlorofluorocarbons. In: Cook PG, Herczeg AL (eds) Environmental tracers in subsurface hydrology. Kluwer, Dordrecht, pp 441–478
42. Barletta B, Meinardi S, Isobel JS, Rowland FS, Chan CY, Wang XM, Zou SC, Chan LY, Donald RB (2006) Ambient halocarbon mixing ratios in 45 Chinese cities. *Atmos Environ* 40(40):7706–7719
43. Plummer LN, Busenberg E, Cook PG (2006) Principles of chlorofluorocarbon dating. In: use of chlorofluorocarbons in hydrology—a guide book. International Atomic Energy Agency, Vienna, pp 17–29
44. Chen ZY, Qi JX, Xu JM, Xu JM, Ye H, Nan YJ (2003) Paleoclimatic interpretation of the past 30 ka from isotopic studies of the deep confined aquifer of the North China Plain. *Appl Geochem* 18(7):997–1009
45. Chen ZY, Nie ZL, Zhang ZJ, Qi JX, Nan YJ (2005) Isotopes and sustainability of ground water resources North China Plain. *Ground Water* 43(4):485–493
46. Zhai YZ, Wang JS, Teng YG, Zuo R (2011) Variations of δ²H and δ¹⁸O in water in Beijing and their implications for the local water cycle. *Resour Sci* 33(1):92–97
47. Michael H, Voss C (2009) Estimation of regional-scale groundwater flow properties in the Bengal Basin of India and Bangladesh. *Hydrogeol J* 17(6):1329–1346
48. Christoph VR, Andreas K, Chen YZ, Rolf K, Werner AH (2010) Characterizing the recharge regime of the strongly exploited aquifers of the North China Plain by environmental tracers. *Water Resour Res.* doi:10.1029/2008WR007660
49. Toth I (2009) Gravitational systems of groundwater flow: theory, evaluation, utilization. Cambridge University Press, Cambridge, p 297